Challenge Journal of STRUCTURAL MECHANICS

Research Article

Investigating Iosipescu shear properties of laser powder bed fusion 316L stainless steel via digital image correlation technique

Elanur Çelebi Kavdır [a], Gürkan Kaya [a,*], Yusuf Polat [a,b]

[a] *Department of Mechanical Engineering, Erzurum Technical University, 25050 Erzurum, Türkiye*
[b] *High Technology Application and Research Center, Erzurum Technical University, 25050 Erzurum, Türkiye*

ABSTRACT

Laser Powder Bed Fusion (LPBF) has been widely adopted for producing stainless steel 316L components with complex geometries; however, despite extensive research on its tensile performance, the shear behavior of LPBF 316L remains insufficiently characterized. Reliable shear properties are crucial for structural components operating under multiaxial loading, yet experimental data enabling accurate calibration of multiaxial yield and failure models are still scarce. In this study, the tensile and shear responses of LPBF 316L were systematically investigated through standard uniaxial tensile testing and Iosipescu shear testing, supported by full-field Digital Image Correlation (DIC). All specimens were fabricated using LPBF system, and their build orientations were precisely documented to account for anisotropy effects. Tensile tests yielded an ultimate tensile strength of approximately 650 MPa and an average elastic modulus of 197 ± 32 GPa. Iosipescu shear tests demonstrated a maximum shear stress of 621 MPa, revealing a notably close relationship between shear strength and tensile strength. The experimentally measured shear modulus was also consistent with the tensile-derived value through classical elastic relations. The combined results deepen our understanding of LPBF 316L mechanical behavior, especially the coupling between tensile and shear responses. The findings further highlight the importance of integrating shear data into design procedures, multiaxial stress assessments, and material databases for additively manufactured stainless steels. Overall, this study provides a robust experimental foundation for improving structural integrity assessments and advancing the design of LPBF 316L components subjected to complex loading.

ARTICLE INFO

Article history:
Received – September 17, 2025
Revision requested – December 1, 2025
Revision received – December 23, 2025
Accepted – December 29, 2025

Keywords:
Laser powder bed fusion
316L stainless steel
Shear strength
Iosipescu test
Digital image correlation

Citation: Çelebi Kavdır E, Kaya G, Polat Y (2026). Investigating Iosipescu shear properties of laser powder bed fusion 316L stainless steel via digital image correlation technique. *Challenge Journal of Structural Mechanics*, 12(1), 45–54.

1. Introduction

Additive manufacturing (AM) enables the production of geometrically complex and material-efficient components directly from digital models (Fidan et al. 2023; Bănică et al. 2024; Ramos et al. 2025). Within metallic AM, laser powder bed fusion (LPBF) is among the most established techniques due to its ability to achieve near-full density, excellent dimensional accuracy, and tailored microstructural features (Drissi-Daoudi et al. 2023). However, the inherent cyclic thermal history of LPBF introduces unique microstructural characteristics, such as cellular or columnar grains, alongside process-related imperfections including porosity and residual stresses. These features strongly influence the resulting mechanical properties, often leading to anisotropy when compared with conventionally manufactured counterparts. As a result, LPBF continues to attract significant research attention, not only for its capacity to manufacture functional end-use components but also for the need to thor-

* *Corresponding author*. E-mail address: gurkan.kaya@erzurum.edu.tr (G. Kaya)
ISSN: 2149-8024 / DOI: https://doi.org/10.20528/cjsmec.2026.01.004

oughly understand the interplay between process, microstructure, and mechanical performance (Gençoğlu et al. 2022; Ismail et al. 2025). Accordingly, robust mechanical characterisation of LPBF materials should be grounded in rigorously validated reference datasets, since incomplete, inconsistent, or non-traceable records can bias property assessment and undermine cross study comparability (Arzomand et al. 2024). In parallel, data driven modelling approaches including machine learning have been increasingly used to infer critical engineering properties from experimental datasets, thereby reducing reliance on labour intensive and time consuming test campaigns while supporting more efficient materials qualification and decision making (More and Kambekar 2025). Moreover, the growing emphasis on timely and non-destructive evaluation has accelerated the use of wireless sensor networks and in situ monitoring frameworks for continuous condition tracking and early anomaly detection; these principles are directly relevant to LPBF process monitoring and NDE based verification pipelines aimed at linking process signatures to resulting mechanical performance (Narwade and Jadhav 2025).

316L stainless steel remains one of the most investigated alloys in LPBF because of its weldability, corrosion resistance, and stable austenitic structure. Its LPBF-processed form typically shows fine microstructural features and mechanical properties comparable to or exceeding those of conventionally processed 316L (Karthik et al. 2021; Sun et al. 2021; Wang et al. 2021; Tang et al. 2022; Drissi-Daoudi et al. 2023). A quantitative comparison of the measured tensile and shear properties with those reported for LPBF 316L shows that the values obtained in this study fall within the typical ranges documented in recent literature. The observed differences can be associated with microstructural variations arising from thermal histories during processing, as also emphasized by (Rottler et al. 2025b), who demonstrated how heat-driven transformations influence mechanical response. Similarly, (Rottler et al. 2025a) on LPBF temperature history highlights the role of heat accumulation and cooling rates in dictating defect formation and microstructural stability, providing context for the mechanical trends observed here. Overall, this comparison confirms that the present tensile–shear dataset is consistent with established LPBF behavior while offering additional insight into shear response, which remains underreported.

The Iosipescu shear test is a widely used method to determine shear properties of metals and composites (Adams 1990; Stojcevski et al. 2018). It provides a full shear stress–strain response and avoids some limitations of alternative techniques such as the short-beam shear test (Allott and Czabaj 2021), off-axis shear test (Gao et al. 2025), and three-rail shear test (May and Kilchert 2022). The specimen features two opposing V-notches at mid-width that produce a reduced cross-section where the shear stress concentrates, enabling controlled shear failure in the central gauge region (Ramezani Dana et al. 2024). For the tensile and compression loading, the notches act as stress concentrations; however, it is negligible for the shear loading. This phenomenon results in a much more uniform shear stress distribution than unnotched shear specimens. In contrast to unnotched geometries, which develop parabolic shear distributions, the Iosipescu geometry provides conditions suitable for accurate determination of shear modulus and shear strength, even for materials with heterogeneous microstructures such as LPBF metals (Liu et al. 2025). In addition to the advantages of the V-notched shear specimen, the DIC method may contribute to capturing displacements of the full-field area under shear loading, which offers a widely validated approach for determining material properties (Jerabek et al. 2010). DIC has also been adapted for in-situ monitoring of large-scale additive manufacturing processes by exploiting the natural surface texture of polymer–composite prints, enabling accurate tracking of full-field deformation and warpage throughout the build (Spencer et al. 2021). Similarly, high-precision full-field deformation measurements in arc-based directed energy deposition have been achieved using both 2D- and 3D-DIC, with results validated against numerical simulations and shown to reliably capture strain evolution despite challenges such as arc light and steep thermal gradients (Wang et al. 2023).

The implementation process of DIC can be summarized in three main steps. First, the surface of the specimen must be prepared with a random speckle pattern. For this purpose, the surface is initially cleaned and coated with a thin white base layer. Once dried, a fine black spray is applied to generate the required random speckle distribution. Following surface preparation, specimens were positioned in the testing apparatus and digital images were captured before and after deformation. Then, the obtained image sets were then processed using correlation algorithms to evaluate displacement and strain fields (Kavdir and Aydin 2019).

Despite growing interest, shear data for LPBF 316L remain scarce, and most applications of the Iosipescu method in metal additive manufacturing have been limited to systematically studying the shear response of LPBF 316L stainless steel. Furthermore, the researchers continue to debate the most suitable approaches for accurately characterizing shear behavior, which underlines the importance of using DIC to validate the strain distribution in the notched region. In this work, we address these gaps by (i) fabricating LPBF 316L Iosipescu specimens and evaluating their as-built shear response with DIC measurement, and (ii) benchmarking the results against co-fabricated tensile specimens to establish a direct comparison between shear and tensile behavior. This combined testing strategy provides a more comprehensive understanding of LPBF 316L under different loading conditions, complementing the tensile-dominated literature and supporting the development of more reliable design data for engineering applications.

In structural applications, most load-bearing components are subjected to complex, multiaxial stress states rather than purely uniaxial tension. Under such conditions, shear stresses often play a dominant role in both yielding and failure initiation. Therefore, reliable shear property data are essential not only for ensuring safe and robust structural design but also for accurately calibrating multiaxial yield criteria such as von Mises, Tresca, and other advanced constitutive models. This

need becomes even more critical for additively manufactured metals like LPBF 316L, whose microstructural heterogeneities, residual stresses, and anisotropy may cause deviations from the behavior of conventionally produced alloys. The scarcity of experimentally validated shear data in the literature thus represents a significant gap that limits the development of dependable design frameworks and material databases for LPBF components. By providing comprehensive shear measurements alongside tensile data, the present study aims to help close this gap and to support more accurate assessment of LPBF 316L under realistic loading conditions.

2. Materials and Methods

In this study, three specimens were prepared for each test type, i.e., tensile and Iosipescu shear tests, in order to determine the corresponding tensile and shear mechanical properties of the LPBF-fabricated material. In addition, strain analyses were performed using the DIC technique to obtain full-field deformation measurements.

DIC was employed to capture full-field deformation and strain data during tensile and Iosipescu shear tests. DIC analyses were carried out in GOM Correlate with subset sizes of 15–25 pixels and step sizes of 10–19 pixels depending on speckle quality and image resolution. Bicubic interpolation and a second-order shape function were used, and correlation was performed with the Zero-Normalized Cross-Correlation criterion. The measurements were carried out with an AVE2 video extensometer attached to the tensile testing machine, equipped with a 16 mm focal length lens. Prior to testing, the specimens (tension and Iosipescu) were prepared with a random speckle pattern by first applying a white base layer and then spraying fine black dots using matte spray paint, as shown in the Figs. 3–5.

2.1. Materials

316L stainless steel powder served as the feedstock material for additive manufacturing via the LPBF method. The particle diameter distribution was determined to be approximately 10–45 μm. Microscopic inspection confirmed that the powder possessed a nearly spherical morphology without agglomeration (see Fig. 1).

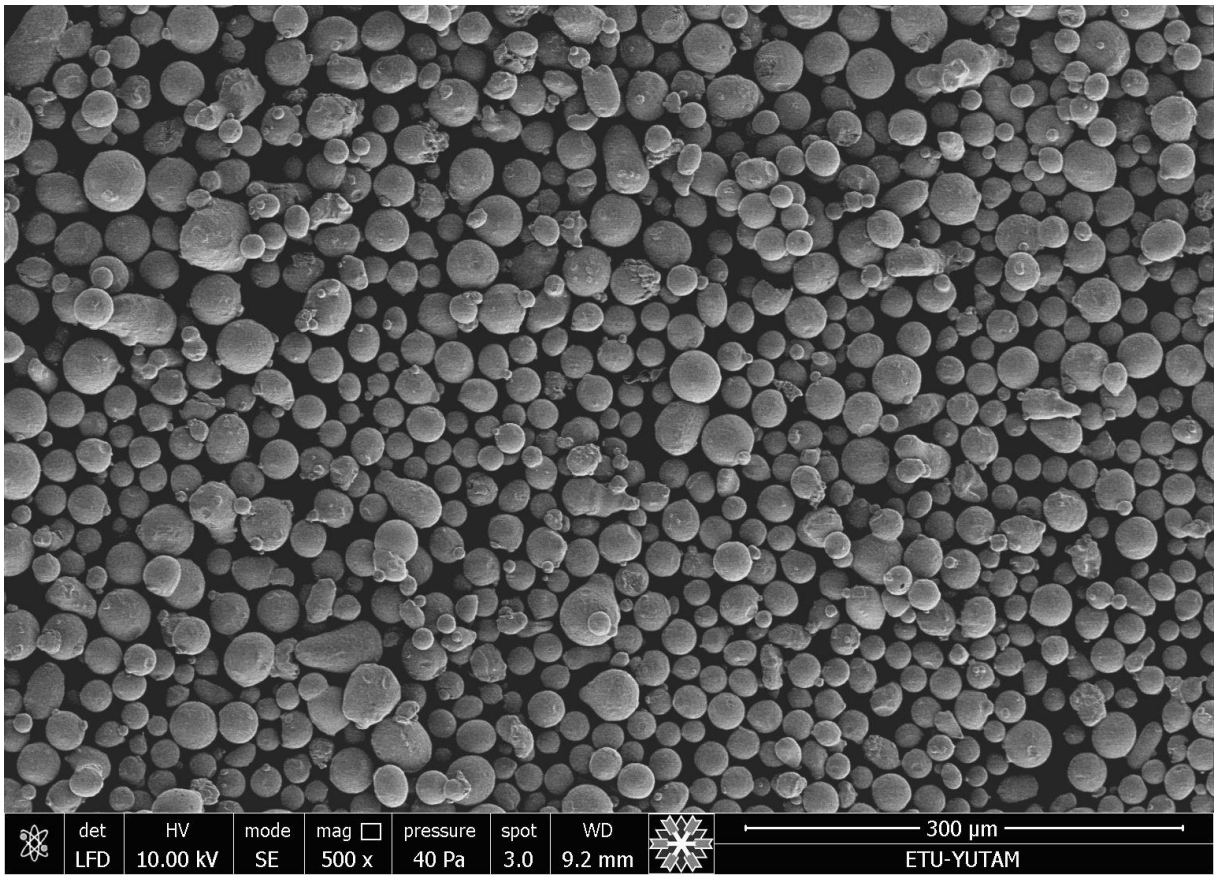

Fig. 1. SEM image of 316L stainless steel powder.

2.2. Laser powder bed fusion technique

Tensile and Iosipescu shear specimens were produced from 316L stainless steel powder using the LPBF technique to evaluate shear behavior. Manufacturing was carried out on a Concept Laser M Lab R system under a nitrogen-protected environment, with oxygen concentration maintained below 1%. The applied process parameters were a laser power of 90 W and a scan speed of 1500 mm/s. The CAD models of the specimens were converted into STL format using AutoFab software. The images of the fabricated specimens are displayed in Fig. 2.

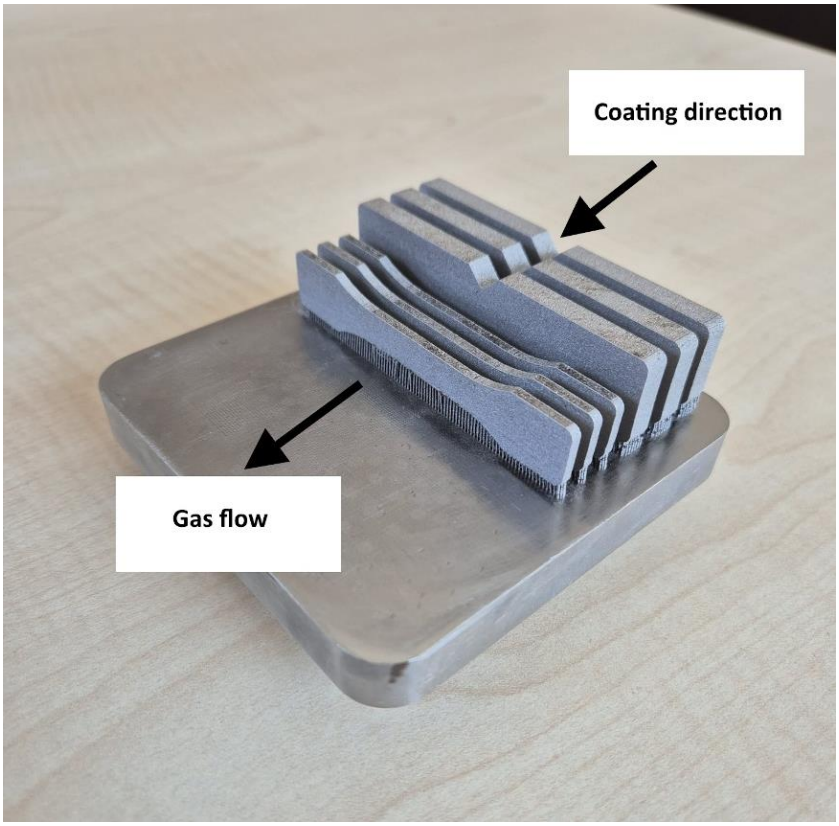

Fig. 2. Tensile and Iosipescu test samples on the LPBF platform.

All specimens were tested in the as-built condition without the application of any thermal post-processing such as stress-relief annealing or hot isostatic pressing (HIP). This choice was made to preserve the intrinsic LPBF microstructure and residual stress state, allowing the shear and tensile behavior to be evaluated directly in the as-fabricated condition.

The production orientation of the test specimens, forces applied during the test and Iosipescu test specimens are given in Fig. 3.

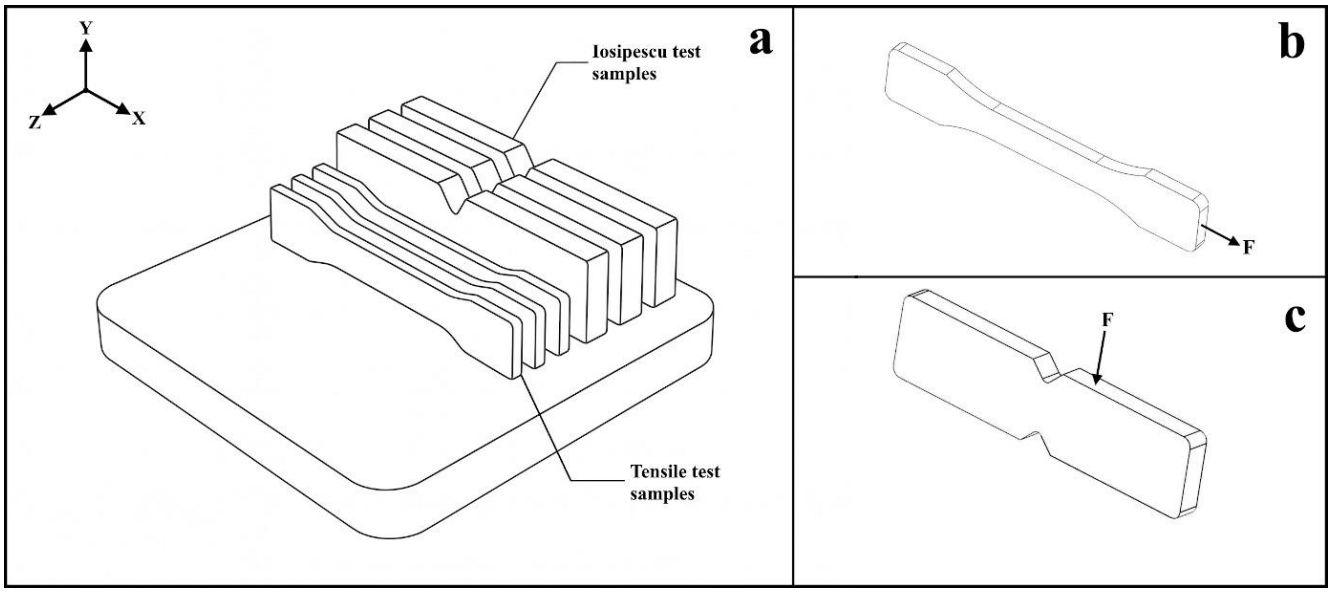

Fig. 3. Schematic representation of the build orientation and specimen alignment for tensile and Iosipescu tests.

2.3. Tensile test

Uniaxial tensile tests were carried out on three specimens using an Instron 5982 static testing machine, as shown in Fig. 4. The specimens were prepared in accordance with standardized geometry (ASTM D638 / ISO 527 type IV dimensions), with an overall length of 75 mm and a thickness of 2 mm. The crosshead displacement rate was set to 1 mm/min throughout the experiments.

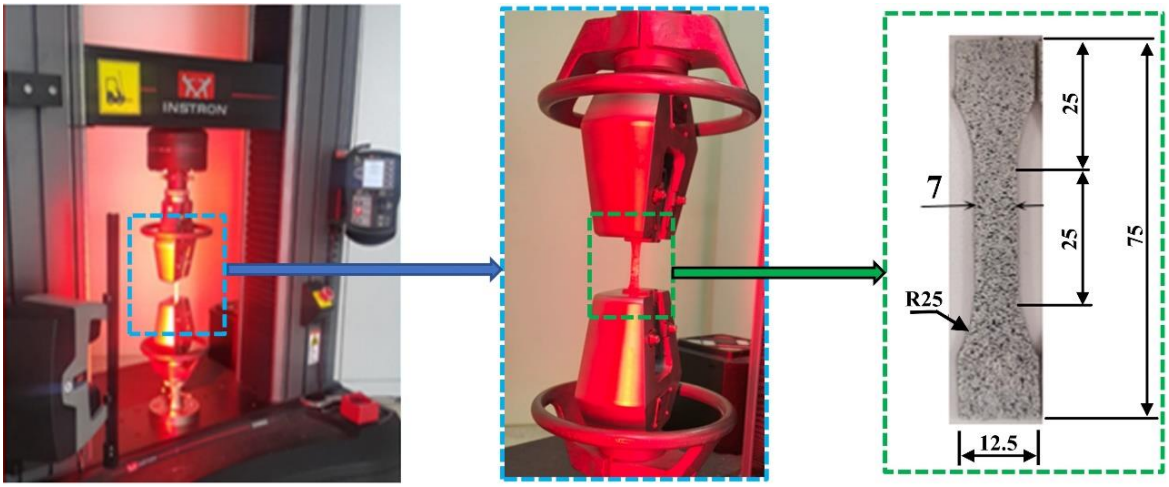

Fig. 4. Experimental setup of the tensile test and geometry of the tensile specimen (dimensions are mm).

The full-field deformation measurements were obtained using the DIC technique, where virtual extensometers (see Fig. 5) were defined along the gauge section to evaluate both axial and lateral strain components. The load–displacement curves were then generated by combining the load data from the load cell with the displacement values measured via DIC. From these curves, the elastic constants (elastic modulus and Poisson's ratio) and the overall stress–strain behavior were determined using the following equations:

$$\sigma_i = P_i/A \tag{1}$$

$$\varepsilon_i = \delta_i/L \tag{2}$$

$$E = \Delta\sigma/\Delta\varepsilon \tag{3}$$

$$\nu = -\Delta\varepsilon_t/\Delta\varepsilon_l \tag{4}$$

where P_i: load value at point i (N), σ_i: normal stress value at point i (MPa), δ_i: displacement value at point i (mm), ε_i: strain value at point i (mm/mm), E: elastic modulus (MPa), ν: Poisson's ratio, L: gauge length (mm), A: cross-sectional area (mm^2) of the specimen.

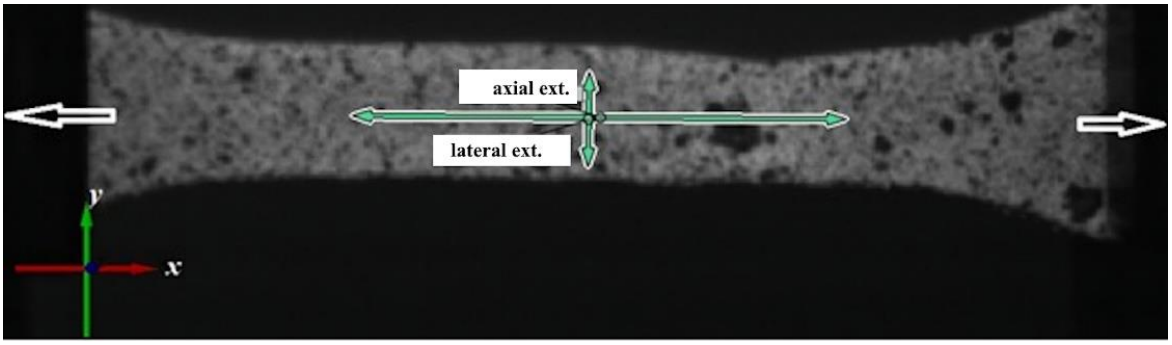

Fig. 5. Representation of the virtual extensometers and coordinate system used in the DIC analysis.

2.4. Iosipescu shear test

The shear properties of the LPBF-fabricated metallic specimens were determined using the Iosipescu shear test in accordance with ASTM D5379/D5379M (V-notched beam method). The experiments were conducted on an Instron 5982 static testing machine at a crosshead displacement rate of 1 mm/min. DIC analysis was employed to determine the shear strain, where virtual extensometers were positioned at ±45° angles within the gauge section. This approach enabled an accurate evaluation of the shear stress–strain response, the in-plane elastic shear modulus, and the shear-related mechanical properties of the material. The specimen geometry and test configuration are presented in Fig. 6.

The shear stress–strain relationship for the Iosipescu specimens was evaluated using the following standard formulations, which enable the determination of shear stress, total shear strain, and shear modulus:

$$\gamma = |\varepsilon_1| + |\varepsilon_2| \tag{5}$$

$$\tau = \frac{F}{tw} \tag{6}$$

$$G = \frac{\tau}{\gamma} \tag{7}$$

In these equations, ε_1 and ε_2: the shear strain components, F: applied force (N), t: specimen thickness (mm), w: specimen width (mm), τ: shear stress (MPa) and γ: total shear strain. The shear modulus is calculated as the ratio of shear stress to shear strain.

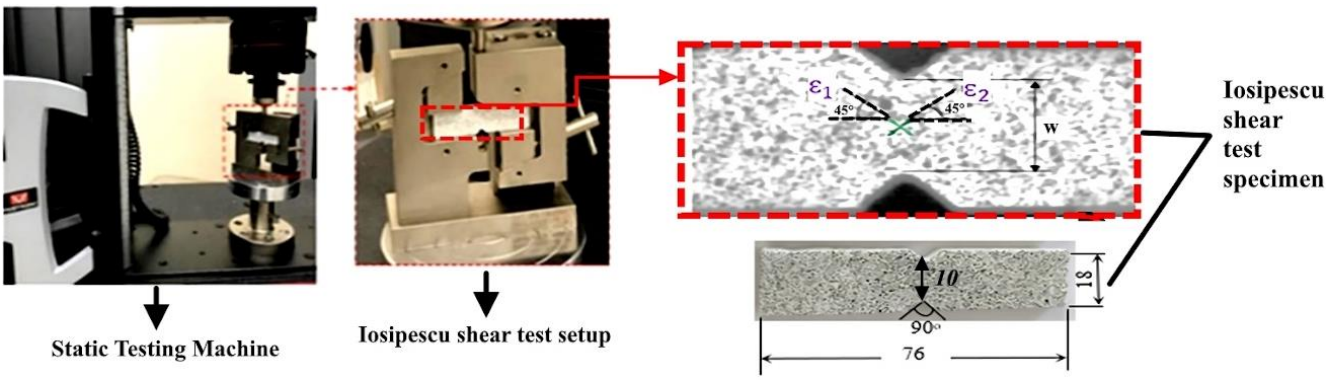

Fig. 6. Specimen geometry and test configuration (dimensions are mm, thickness 5 mm).

3. Results and Discussion

3.1. Tensile test results

The mechanical properties of the three specimens, including true stress, strain, Poisson's ratio, and elastic modulus, are summarized in Table 1 (E: Modulus of elasticity; ν: Poisson's ratio; σ_u: Ultimate strength; ε_{f_a}: Maximum axial strain; ε_{f_l}: Maximum lateral strain). In addition, the Fig. 7 presents the engineering stress-strain curves obtained for each tested specimen.

Table 1. Tensile test results.

Properties	Mean value (±SD)
E (GPa)	197.1 ± 32.1
ν	0.326 ± 0.096
σ_u (MPa)	649.6 ± 7.4
ε_{f_a}	0.243 ± 0.096
ε_{f_l}	−0.085 ± 0.038

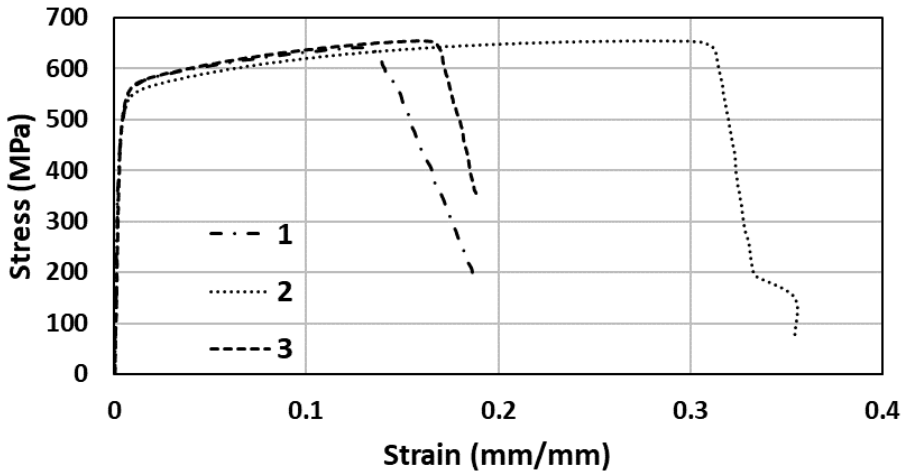

Fig. 7. The engineering stress-strain curves for tensile test specimens.

The tensile test results revealed that the LPBF-fabricated metallic specimens exhibited a highly consistent tensile strength, with an average ultimate stress of 649.6 ± 7.4 MPa. In contrast, noticeable variations were observed in the elastic modulus (197.1 ± 32.1 GPa) and strain values, indicating heterogeneity in stiffness and ductility among the specimens. The stress–strain curves (Fig. 7) confirmed these findings, showing similar maximum stress levels but different slopes in the elastic region and varying strain-to-failure values. These differences are likely related to microstructural heterogeneities or process-induced defects inherent to the additive manufacturing process. Overall, the results suggest that while tensile strength is reproducible and reliable, further optimization of the LPBF process parameters is required to achieve more uniform stiffness and ductility.

The evolution of the damage process during tensile loading was captured by the DIC strain maps presented along with the stress–strain curve (see Fig. 8). Here, (a) represents the initial state without load and no elongation, (b) corresponds to $\varepsilon \approx 0.09$, (c) to $\varepsilon \approx 0.23$, and (d) to $\varepsilon \approx 0.33$, showing the normal strain distributions along the loading direction. At the initial stage, the axial strain distribution was relatively homogeneous throughout the gauge section, indicating uniform elastic and early plastic deformation. As the applied strain increased, strain gradients became more pronounced and the onset of localized deformation could be observed, reflecting the initiation of necking in the specimen. At the later stage, strain localization intensified significantly, with the highest strain values concentrated within a narrow band that corresponded to the eventual fracture site. This evo-

lution demonstrates a transition from diffuse plastic deformation to localized necking, followed by fracture, which is consistent with the post-peak softening observed in the stress–strain response. Such results highlight the capability of DIC to provide full-field insights into the deformation and failure mechanisms of additively manufactured metallic materials under tensile loading.

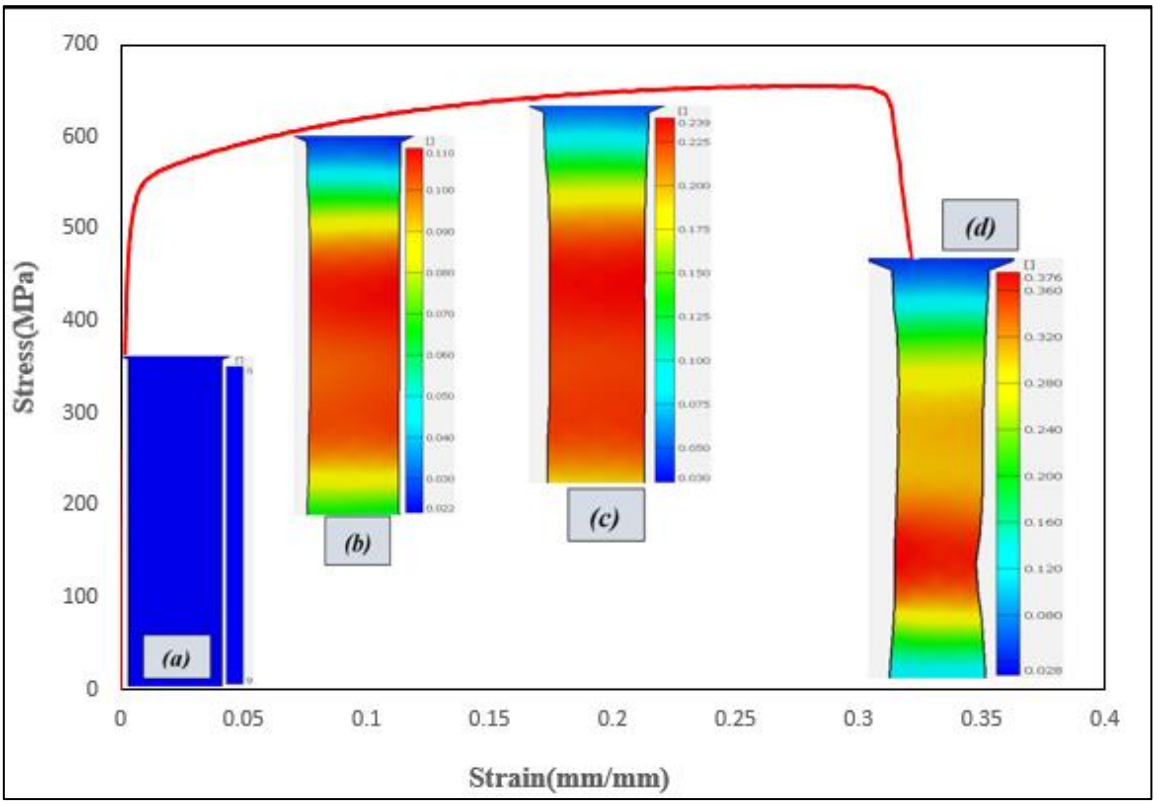

Fig. 8. Engineering stress–strain curve of the tensile specimen with corresponding DIC normal strain maps at different loading stages.

3.2. Iosipescu shear test results

Three Iosipescu specimens were tested under shear loading, and the experimental results are presented in Table 2 (G: Shear modulus; τ_f: Maximum shear stress; γ_f: Maximum shear strain), and the shear stress-strain curves are given in Fig 9.

Table 2. Iosipescu shear test results.

Properties	Mean value (±SD)
G (GPa)	72.0 ± 2.6
τ_f (MPa)	621.2 ± 21.1
γ_f	0.577 ± 0.045

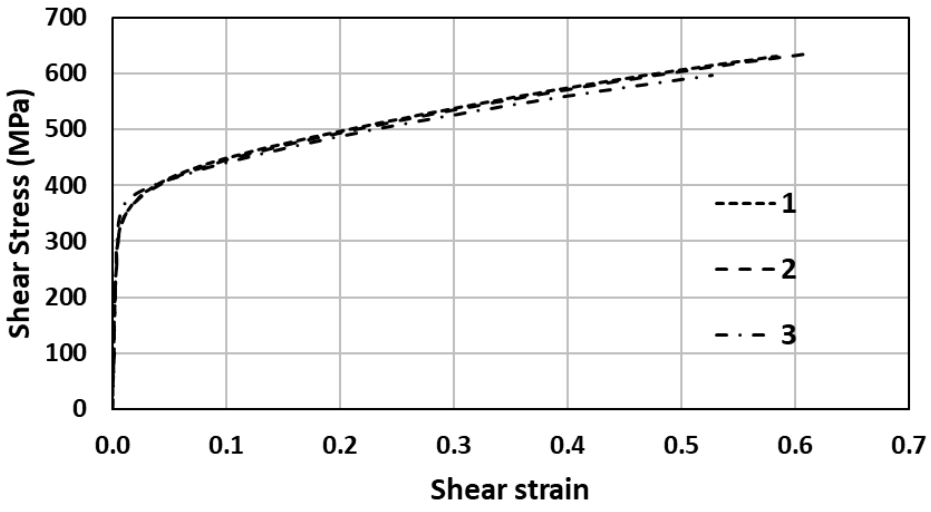

Fig. 9. The engineering shear stress-strain curves for Iosipescu test specimens.

The Iosipescu shear test results of the LPBF-fabricated specimens demonstrated highly consistent behavior among the three samples. The average shear modulus was calculated as 72.0 ± 2.6 GPa, indicating good agreement of stiffness values across the specimens. Similarly, the maximum shear stress (621.2 ± 21.1 MPa) showed a very narrow scatter, confirming the reliability and repeatability of the shear strength. The maximum shear strain was determined as 0.577 ± 0.045, suggesting that the ductility of the material also followed a consistent trend. The shear stress–strain curves nearly overlapped, further verifying the uniformity of the experimental results. In particular, the elastic region slopes were well aligned with the calculated shear modulus values, while the peak stresses and strain-to-failure levels revealed no significant deviation among the specimens. Overall, these results emphasize that the shear response of additively manufactured metallic materials is not only reproducible but also homogeneous in terms of stiffness, strength, and ductility, which underlines the reliability of the applied methodology.

The maximum shear stress obtained from the Iosipescu tests (≈ 621 MPa) is in close agreement with the ultimate tensile strength (≈ 650 MPa). This correspondence is noteworthy in the context of multiaxial yield criteria. While von Mises and Tresca predict shear yield stresses of $\sigma_y/\sqrt{3}$ and $\sigma_y/2$, respectively, the experimental results suggest a shear resistance approaching the tensile strength. Such behavior highlights the unique microstructural response of LPBF 316L and provides a useful reference point for calibrating multiaxial constitutive models and failure criteria in additively manufactured metals.

Fig. 10 presents the shear strain distributions of the Iosipescu specimen at different loading stages. These strain maps clearly illustrate the evolution of deformation and the formation of a pure shear strain field in the central gauge section. Although there are only a limited number of studies addressing the shear properties of metallic materials using the Iosipescu test, the present results confirm the suitability of this method. The consistency observed among the specimens, together with the DIC-based strain maps, demonstrates that the expected shear strain field was successfully generated, which is essential for accurately determining shear mechanical properties. This gap underscores, DIC provided full-field strain data that cannot be captured through conventional deformation measurement techniques, thus validating both the accuracy of the Iosipescu test and the reliability of the experimental procedure. Overall, the combination of Iosipescu testing and DIC analysis offers a powerful approach for the comprehensive characterization of shear behavior in additively manufactured metallic materials.

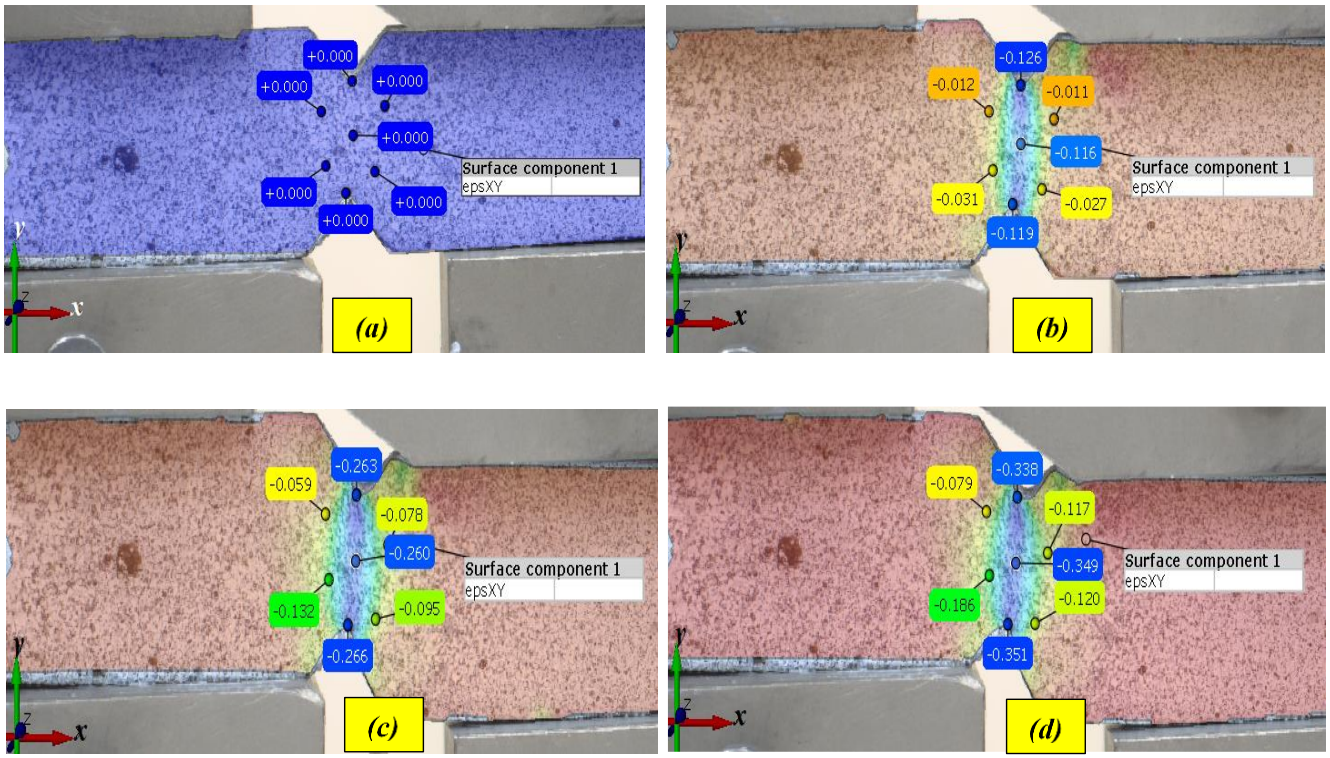

Fig. 10. Evolution of shear strain distribution in the Iosipescu specimen at different loading stages: (a) γ = 0; (b) γ = 0.189; (c) γ = 0.456; (d) γ = 0.604.

4. Conclusions

In this study, the tensile and shear properties of 316L stainless steel fabricated by laser powder bed fusion were systematically investigated using the digital image correlation technique. Particular emphasis was placed on characterizing the multiaxial mechanical response, with a focus on shear behavior, which has been scarcely reported for LPBF 316L alloys. The application of DIC enabled full-field strain and displacement measurements, thereby improving the accuracy and reliability of the extracted elastic modulus, shear modulus, and Poisson's ratio.

The experimental results revealed that the LPBF-fabricated specimens exhibited a consistent ultimate tensile strength of 649.6 ± 7.4 MPa, with an average elastic modulus of 197.1 ± 32.1 GPa. Under shear loading, the Iosipescu tests yielded an average shear modulus of 72.0 ± 2.6 GPa and a maximum shear stress of 621.2 ± 21.1 MPa, demonstrating excellent reproducibility and uniformity. The uniform strain distribution observed within the gauge section confirmed that the V-notched Iosipescu method, in combination with DIC, provides a robust and reliable approach for capturing the pure shear stress–strain response.

A key outcome of this work is the close alignment between the tensile and shear strengths, which provides valuable insight into the governing deformation mechanisms of LPBF 316L. This relationship also offers a practical advantage for calibrating multiaxial yield and failure criteria such as von Mises and Tresca, both of which require accurate shear and tensile limits for reliable predictions. The results demonstrate that LPBF 316L exhibits a more uniform strength response under different loading modes than is often assumed, emphasizing the importance of incorporating shear data when evaluating the structural integrity of additively manufactured components.

The combined tensile and shear data obtained in this study offer direct input for engineering design frameworks, particularly those requiring reliable multiaxial material parameters for LPBF 316L. The close correspondence between tensile and shear strengths, together with the experimentally validated shear modulus, enables more accurate calibration of commonly used design criteria such as von Mises and Tresca, as well as improved selection of safety factors for components subjected to complex loading. These experimentally derived properties can also serve as dependable entries for material databases used in design and simulation workflows, thereby supporting more robust structural integrity assessments for LPBF-fabricated 316L components.

The results obtained in this study also have practical implications for the structural design of LPBF 316L components. Since most load-bearing parts operate under multiaxial stress states, the experimentally determined tensile and shear properties — particularly the close values of tensile and shear strength and the validated shear modulus — can serve as reliable input for calibrating multiaxial yield and failure criteria. These data provide a more robust basis for material selection, safety-factor determination, and the development of design databases for additively manufactured 316L structures.

Overall, this work contributes to filling a significant gap in the literature by establishing reliable shear property data for as-built LPBF 316L stainless steel. The outcomes not only enhance the understanding of the material's multiaxial mechanical behavior under complex loading conditions but also provide critical input for the reliable design and structural application of LPBF-fabricated components. In addition to conclusion of this study, a post-treatment study may contribute to the improvement of microstructure of as-built LPBF samples for further tensile and shear properties.

Acknowledgements

The authors would like to thank High Technology Research Center (ETÜ-YÜTAM), Erzurum Technical University because of their support in the experimental stages.

Funding

The authors received no financial support for the research, authorship, and/or publication of this manuscript.

Conflict of Interest

The authors declare no potential conflicts of interest with respect to the research, authorship, and/or publication of this manuscript.

Data Availability

The datasets generated and/or analyzed during the current study are not publicly available but are available from the corresponding author upon reasonable request.

AI Assistance

No AI-based tools were used in the preparation of this manuscript.

Author Contributions

All authors made substantial contributions to the conception and design of the study, acquisition of data, analysis and interpretation of data; drafted or critically revised the manuscript for important intellectual content; and approved the final version to be published.

REFERENCES

Adams DF (1990). The Iosipescu shear test method as used for testing polymers and composite materials. *Polymer Composites*, 11(5), 286–290.

Allott NR, Czabaj MW (2021). Characterization of the interlaminar shear strength of IM7/8552 using small-scale short beam shear tests. *Composites Part A: Applied Science and Manufacturing*, 142, 106200.

Arzomand K, Rustell M, Kalganova T (2024). From ruins to reconstruction: Harnessing text-to-image AI for restoring historical architectures. *Challenge Journal of Structural Mechanics*, 10(2), 69-85.

Bănică CF, Sover A, Anghel DC (2024). Printing the future layer by layer: A comprehensive exploration of additive manufacturing in the era of Industry 4.0. *Applied Sciences*, 14(21), 9919.

Drissi-Daoudi R, Masinelli G, de Formanoir C, Wasmer K, Jhabvala J, Logé RE (2023). Acoustic emission for the prediction of processing regimes in laser powder bed fusion, and the generation of processing maps. *Additive Manufacturing*, 67, 103484.

Fidan I, Huseynov O, Ali MA, Alkunte S, Rajeshirke M, Gupta A, Hasanov S, Tantawi K, Yasa E, Yilmaz O, Loy J, Popov V, Sharma A (2023). Recent inventions in additive manufacturing: Holistic review. *Inventions*, 8(4), 103.

Gao Q, Zhao X, Sun Q (2025). Evaluation of the off-axis and on-axis tensile creep behavior of glass-fiber reinforced polymer unidirectional lamina. *Polymer Composites*, 46(4), 3054–3069.

Gençoğlu U, Kaya G, Ergüder TO, Hacısalihoğlu İ, Yıldız F (2022). Investigation of the structural and tribological properties of 316L stainless steel manufactured using variable production parameters by selective laser melting. *Journal of Materials Engineering and Performance*, 31(5), 3688–3703.

Ismail L, Mohamed OF, Farrah T, George P, Schiffer A (2025). Influence of process parameters on microstructure and interfacial mechanical properties of Al6061/AlSi10Mg multi-material components fabricated via laser powder bed fusion. *Materials Science and Engineering: A*, 928, 148061.

Jerabek M, Major Z, Lang RW (2010). Strain determination of polymeric materials using digital image correlation. *Polymer Testing*, 29(3), 407–416.

Karthik GM, Kim ES, Sathiyamoorthi P, Zargaran A, Jeong SG, Xiong R, Kang SH, Cho JW, Kim HS (2021). Delayed deformation-induced martensite transformation and enhanced cryogenic tensile properties in laser additive manufactured 316L austenitic stainless steel. *Additive Manufacturing*, 47, 102314.

Kavdir EÇ, Aydin MD (2019). The investigation of mechanical properties of a structural adhesive via digital image correlation (DIC) technic. *Composites Part B: Engineering*, 173, 106995.

Liu Z, Wang J, Sun W, Liu X, Gao Z, Li J, Zhan X (2025). Unveiling the dependence of mechanical properties and corrosion resistance on microstructural heterogeneity in additively manufactured 316L stainless steel. *Journal of Materials Research and Technology*, 37, 4688–4707.

May M, Kilchert S (2022). The effect of loading rate on the in-plane shear strength of tri-axial braided composites. *Journal of Composite Materials*, 56(3), 421–426.

More S, Kambekar A (2025). Performance evaluation of compressive strength of concrete using different machine learning algorithms. *Challenge Journal of Concrete Research Letters*, 16(2), 60-68.

Narwade R, Jadhav R (2025). Concrete strength monitoring and damage detection using piezoelectric-based wireless sensor. *Challenge Journal of Concrete Research Letters*, 16(1), 40-50.

Ramezani Dana H, El Mansori M, Contreras Echevarria A, Muñoz Basagoiti MX, Pisarski M, Cucuzzella F, Sansone C (2024). Determination of shear strength of additively manufactured poly lactic acid/flax fibre bio-composite via the iosipescu test. *Composites Communications*, 47, 101858.

Ramos A, Angel VG, Siqueiros M, Sahagun T, Gonzalez L, Ballesteros R (2025). Reviewing additive manufacturing techniques: Material trends and weight optimization possibilities through innovative printing patterns. *Materials*, 18(6), 1377.

Rottler J, Tetzlaff TK, Lion A, Paetzold-Byhain K, Johlitz M (2025a). Temperature history in laser powder bed fusion: Analyzing the effect of heat accumulation on the microstructural state of Ti-6Al-4V. In: Altenbach, H., Hitzler, L., Johlitz, M., Merkel, M., Öchsner, A. (eds) *Lectures Notes on Advanced Structured Materials 3*. Advanced Structured Materials, vol 226. Springer, Cham.

Rottler J, Tetzlaff TK, Wohninsland A, Lion A, Johlitz M (2025b). Thermophysical and microstructural characterization of Ti-6Al-4V in powder and laser powder bed fusion-processed state within the global temperature field range. *Materials and Design*, 253, 113823.

Spencer R, Hassen AA, Baba J, Lindahl J, Love L, Kunc V, Babu S, Vaidya U (2021). An innovative digital image correlation technique for in-situ process monitoring of composite structures in large scale additive manufacturing. *Composite Structures*, 276, 114545.

Stojcevski F, Hilditch T, Henderson LC (2018). A modern account of Iosipescu testing. *Composites Part A: Applied Science and Manufacturing*, 107, 545–554.

Sun C, Wang Y, McMurtrey MD, Jerred ND, Liou F, Li J (2021). Additive manufacturing for energy: A review. *Applied Energy*, 282, 116041.

Tang L, Magdysyuk OV, Jiang F, Wang Y, Evans A, Kabra S, Cai B (2022). Mechanical performance and deformation mechanisms at cryogenic temperatures of 316L stainless steel processed by laser powder bed fusion: In situ neutron diffraction. *Scripta Materialia*, 218, 114806.

Wang Q, Jia J, Zhao Y, Wu A (2023). In situ measurement of full-field deformation for arc-based directed energy deposition via digital image correlation technology. *Additive Manufacturing*, 72, 103635.

Wang X, Sanchez-Mata O, Atabay SE, Muñiz-Lerma JA, Attarian Shandiz M, Brochu M (2021). Crystallographic orientation dependence of Charpy impact behaviours in stainless steel 316L fabricated by laser powder bed fusion. *Additive Manufacturing*, 46, 102104.